

SIXTH EUROPEAN ROTORCRAFT AND POWERED LIFT AIRCRAFT FORUM

Paper No. 59

**RESEARCH INTO A HELICOPTER ROTOR'S
SPEED AND LOAD FACTOR LIMITS**

B. CERTAIN & J.M. BESSE

Société Nationale Industrielle Aérospatiale

Helicopter Division

Marignane, France

September 16 -19, 1980

Bristol, England

THE UNIVERSITY, BRISTOL, BS8 1HR, ENGLAND

RESEARCH INTO A HELICOPTER ROTOR'S SPEED AND LOAD FACTOR LIMITS

B. CERTAIN & J.M. BESSE

Société Nationale Industrielle Aérospatiale

1 – INTRODUCTION

The main rotor has always been the prime cause of most of the helicopter's flight envelope limitations.

The loads applied to the rotor have increased further on modern helicopters, for a variety of reasons :

- The high level of installed power due to twin-engined design and to the concern to maintain adequate performance after an engine failure during take-off, in hot weather or at high altitude.
- High forward speeds resulting from the increase in power, of course, but also from great improvements in the aerodynamic efficiency of the fuselage achieved mainly by the use of retractable landing gear and rotor mast fairing.
- High rotor loads made possible by the power reserve.

In addition, there have been major technological developments which enable the rotor mast, head and blade assemblies to bear high levels of stress ; these are of course the use of glass and carbon fibres, laminated hinges and viscoelastic dampers.

This almost systematic attempt to push normal performance to the aerodynamic limits of the airfoils has posed new theoretical problems (unsteady aerodynamics) and also problems of testing methodology, since the behaviour of the new blade profiles is relatively new ground alongside that of the "old faithful" NACA 0012, which was used for all our helicopters until quite recently.

Using the example of the SA 365N, known as the «Coast Guard» Dauphin (2 x 440 kW twin-engined helicopter which can do 160 kt in level flight at sea level, at its maximum weight of 3 800 kg), let us briefly recall the origins of the "barriers" limiting the helicopter's flight envelope. After that we will describe the equipment used for measurement, in-flight monitoring and processing and analysis of data. Lastly, we will describe the testing method and see a film taken during flights at the limit of the flight envelope.

2 – PHYSICAL PHENOMENA CAUSING LIMITATIONS

2.1 – Stall

This is the classic problem posed by the retreating blade, which must maintain some lift while its relative airspeed becomes low and may reach zero towards the centre (reverse flow circle).

The angle of attack increases and the pitch change rods are subjected to high stress.

Fig. 1 shows the pattern of this signal, reflecting the load factor, on the first generation of 365N blades.

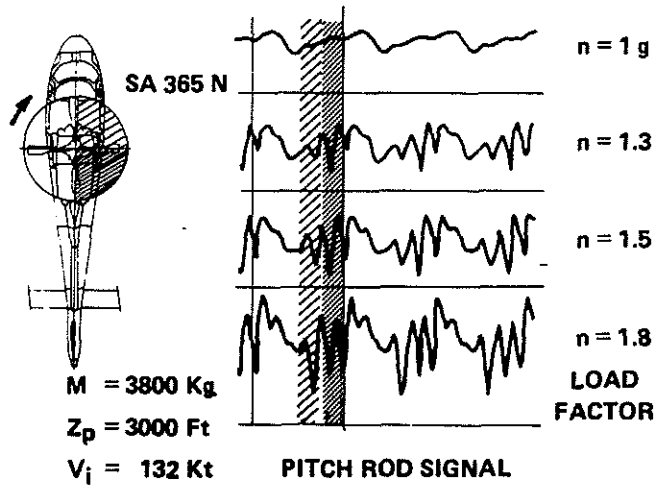


Figure 1 : STALL FLUTTER

We see that the divergence becomes visible with the blade in the forward position, goes into the yellow range and begins to fall in the middle of the red range, i.e. with the blade in the 3/4 position rearwards.

On the signal, which for $n = 1g$ is almost pure 1Ω , there is superimposed a strong 6Ω modulation which corresponds to a torsional mode response in the blade.

Fig. 2 gives a schematic explanation of this phenomenon, which is known as "stall flutter".

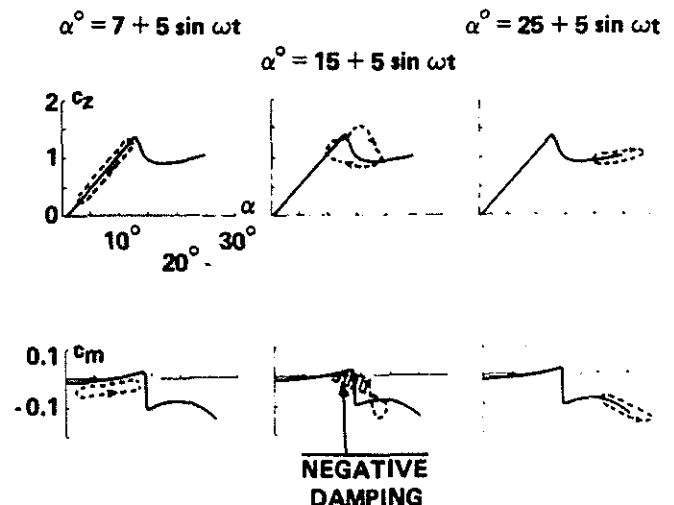


Figure 2 : UNSTEADY CHARACTERISTICS

The continuous curves represent the polar graph of a blade profile tested in the wind-tunnel ($C_z = f(\alpha) - C_m = f(\alpha)$).

The dotted curves are the unsteady polar graphs, in other words the relations between lift and moment while the profile's angle of attack oscillates by $\pm 5^\circ$ around an average value.

Without going into detail, we can state that the stall angle is no longer fixed, but it depends on the speed of variation of the angle of attack ; stalling is delayed when the angle of attack increases, and persists all the more when the angle of attack decreases rapidly.

The helicopter's operational conditions correspond to the first two cases ($\alpha = 7 + 5 \sin \Omega t$ and $\alpha = 15 + 5 \sin \Omega t$). In the latter, we note a curious pattern of $C_m = f(\alpha)$, shaped like an 8, and it is shown that in the shaded area the damping is negative and the profile absorbs energy from the airflow. Also, we observe that this phenomenon occurs at the low incidence areas in the cycle ; this is shown by the pitch rod signal on fig. 1, which starts to diverge when the blade is in the forward position, while the angle of attack is still low, and to converge in an area where it is still high.

This phenomenon is never divergent since there is positive damping over one cycle, but it may create very high stresses by excitation of the first natural torsional frequency.

A solution to this problem has been found, consisting of centering the blade tip further forward. The increased twist in the retreating blade caused by this increase in the zero pitch return moment considerably reduces the blade tip incidence.

2.2 – Limit Mach Number

The advancing blade tip can reach a high Mach number, giving rise to transonic effects, namely a rapid increase in drag and the development of moments due to rearward displacement of the blade's aerodynamic centre.

Fig. 3 demonstrates the complexity of this problem by reference to 4 parameters :

- (1) Viscoelastic drag damper stress
- (2) Drag stress at blade root
- (3) Blade root flapping
- (4) Pitch change rod stress

In this flight phase the Mach number is close to 0.97, and the blade profile used is OA 209.

We observe a high modulation in drag at a frequency of $\Omega/2$ and a high variation in the pitch change rod signal at the limit of the shaded areas only for the advancing blade. The latter signal is also at a frequency of $\Omega/2$, and clearly the phenomenon only occurs one time per two revolutions.

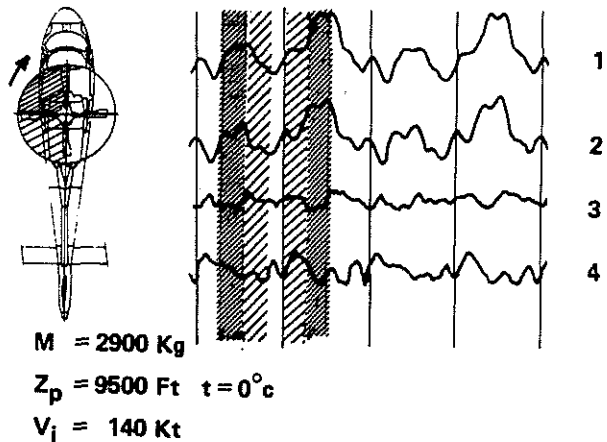


Figure 3 : LIMIT MACH NUMBER

This throws the rotor out of track, since each blade has two paths which it follows alternately.

From the cabin, the rotor appears to have a will of its own. Here again, the stresses can reach very high levels.

Special attention has been paid to blade profiles with a view to delaying this phenomenon ; fig. 4 gives some comparative results, the reference profile being NACA 0012.

A profile is characterized by the Mach number at which the drag gradient dC_x/dM reaches 0.1.

The left-hand side of fig. 4 gives the critical Mach number at zero lift ; we see that NACA 0012 reaches 0.8, the SA 131 type (PUMA) blade profiles go up to 0.85 and the OA2 line to 0.87. Note the important effect of relative thickness.

The right-hand side shows the same criteria with positive lift. The modern blade profiles maintain an advantage up to about 0.3 C_z .

Although these airfoil improvements are very significant (and reflected in performance), they are not sufficient to cover the flight envelope claimed today by the most recent helicopters. Work was done on developing the blade tip using swept-back tips, which do not serve the same purpose as the wing sweep on an aeroplane but create a centre of pressure to the rear of the twisting axis, stabilizing the blade and reducing the twisting variations caused by aerodynamic forces.

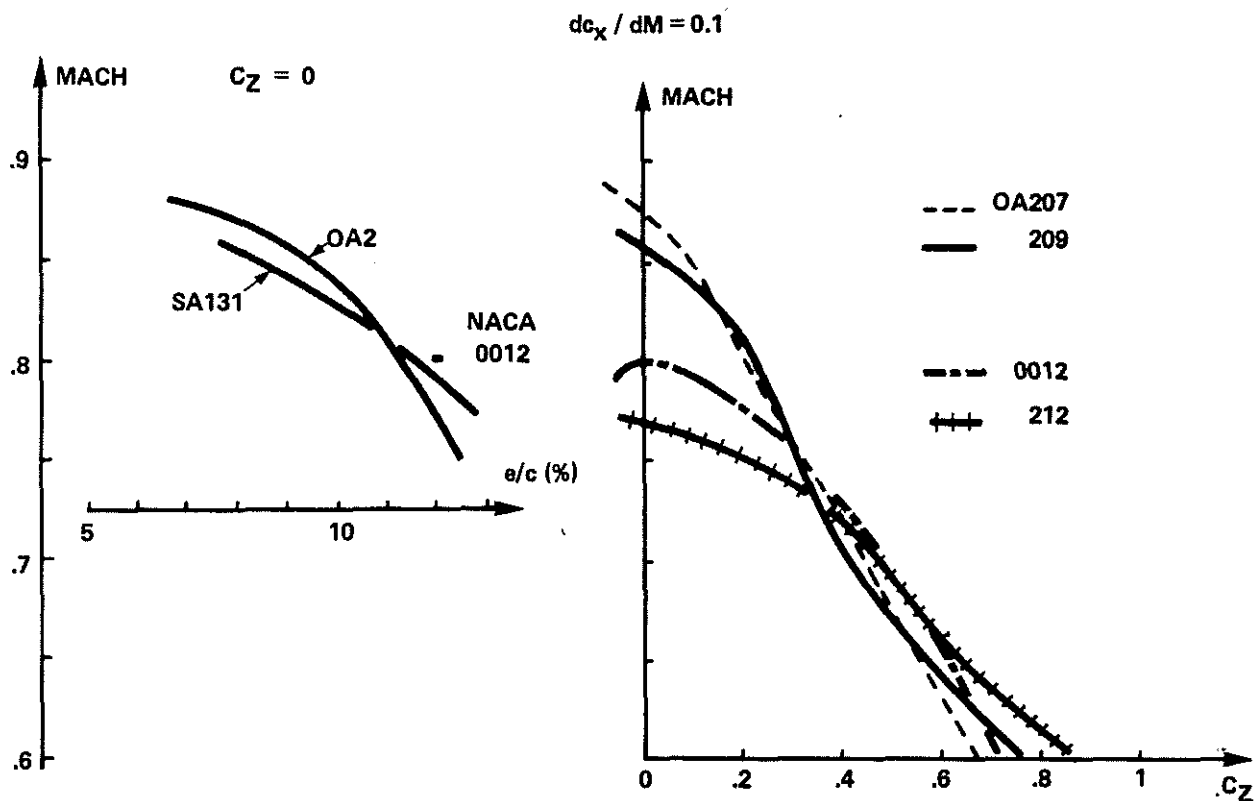


Figure 4 : BLADE PROFILE CHARACTERISTICS

3 – TEST FACILITIES

It is apparent from this brief review that certain stress levels must be monitored in flight, to warn the crew when there are imminent phenomena that, when triggered off, are fairly violent if not actually explosive.

Also, these increases in stress levels are generally not perceptible by vibrations inside the helicopter until these phenomena have firmly set in. Help from telemetry is thus essential.

Aside from its monitoring role, the airborne test equipment is used to record a large number of vibration and stress parameters, as well as all the slowly-changing flight parameters, which are processed numerically (P.C.M.).

On the ground, this mass of data is processed and analyzed, both during the test flight and afterwards.

Figs. 5 to 16 will help to describe this type of test equipment ; the example shown is still the AS 365N.

3.1 – Airborne test installation

Photographs 5 and 6 show a Starflex rotor head fitted with the gauges and a slip-ring with about 40 tracks for recording stresses in the blades (flapping and lagging stresses), in the pitch change rods, in the rotor hub arms and centre part, and displacements of frequency adapters, rotor shaft bending, signals from 3-component accelerometers on the rotor head, etc ...

These measurements, together with those from the airframe and tail rotor, are transmitted to a rack whose layout is given in fig. 7. They are calibrated in a series of amplifiers. There is a mixing panel so that each track can be directed to one of the 12 channels of the 8 multiplex units.

Actually, the choice of the position is not arbitrary, because all channels do not have the same pass band.

(The pass band for each track is proportional to the frequency of the corresponding sub-carrier. These are spaced so as to separate information when the tracks are combined, and so that it is possible to reconstitute it by filtering when the tape is run).

The mixed signals are then magnetically recorded together with a time base signal, as also the conversations between the crew and telemetry post.

Some of the data can be displayed on the aircraft display scopes (mainly on the larger helicopters), but 12 tracks are sent to the ground telemetry unit by a transmitter (20 W Band P).

Figure 8 shows this testing installation on board the 365N ; on the left we see the magnetic recorder, on the right the amplifiers. See also figure 9.

The total airborne equipment, including wiring and the P.C.M. unit, weights about 250 kg.

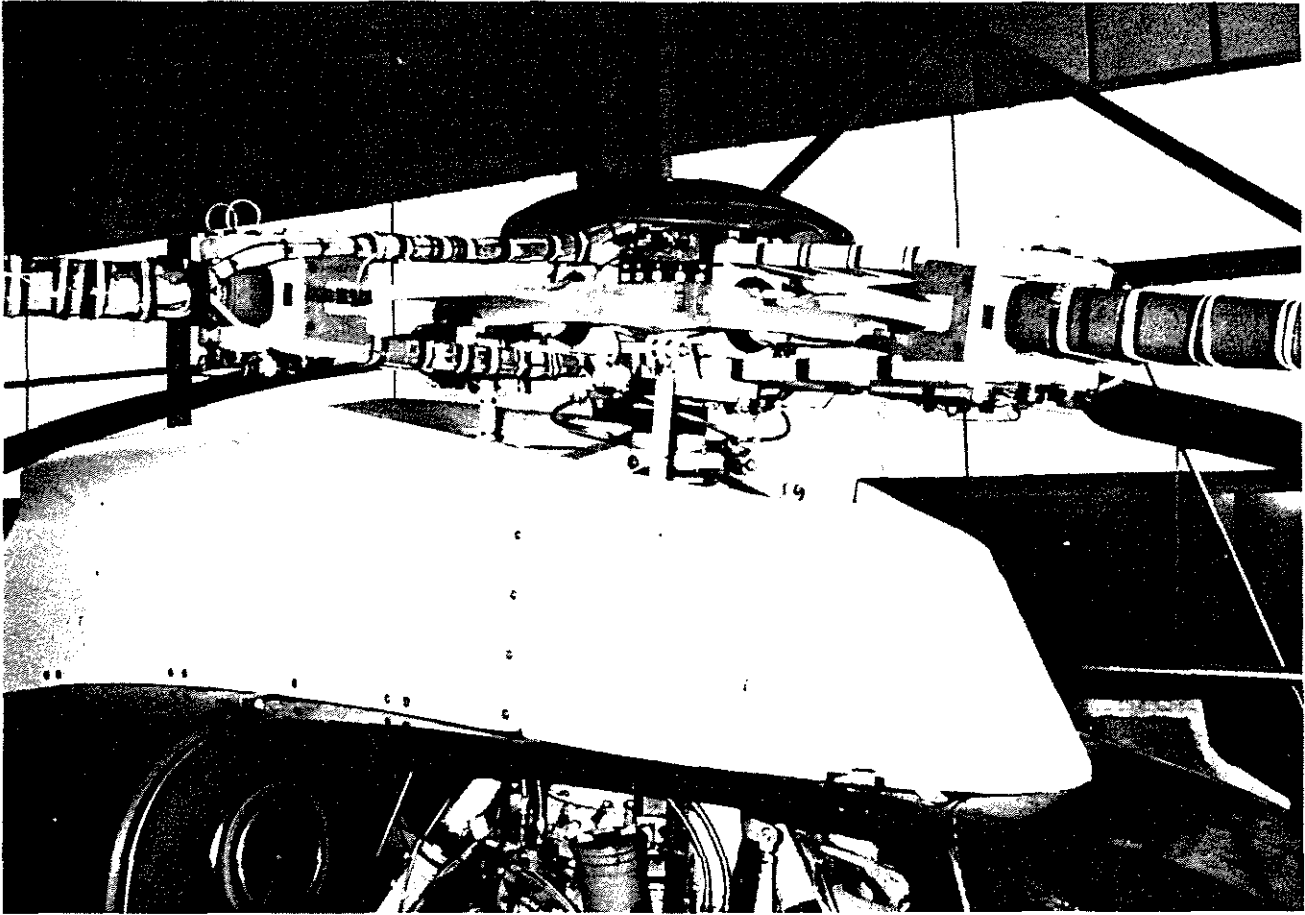


Figure 5 : COWLING AND STARFLEX ROTOR HEAD

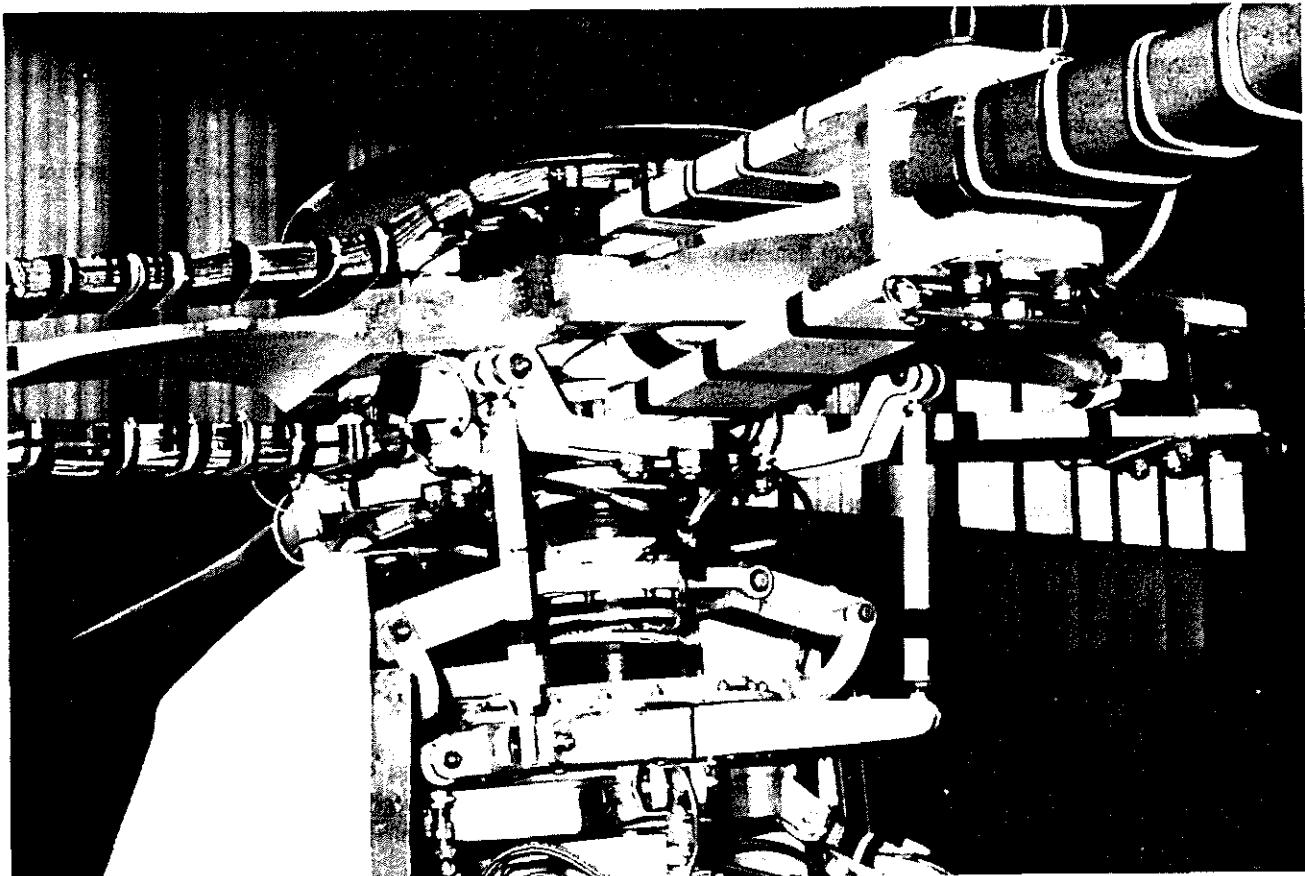


Figure 6 : STARFLEX ROTOR HEAD WITH STRAIN GAUGES

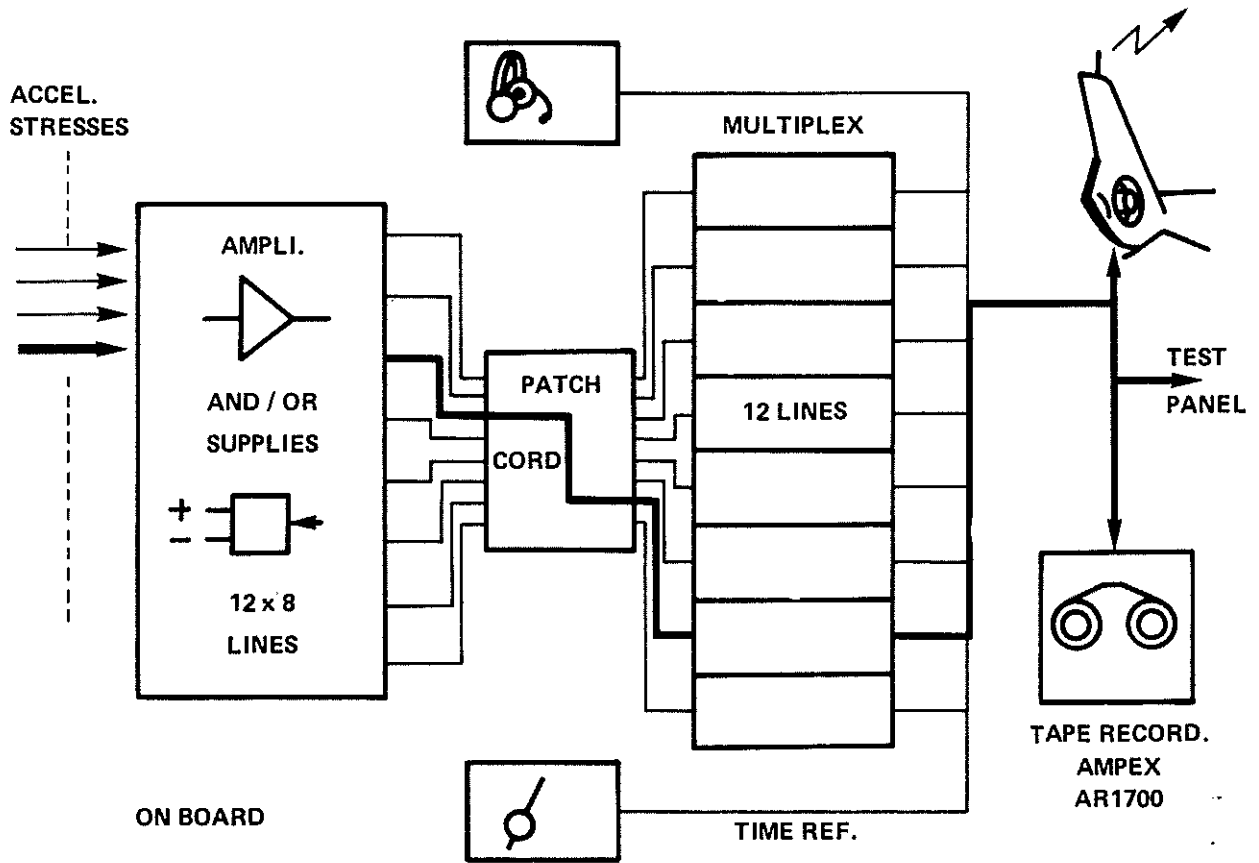


Figure 7 : BLOCK DIAGRAM OF TEST EQUIPMENT IN AIRCRAFT

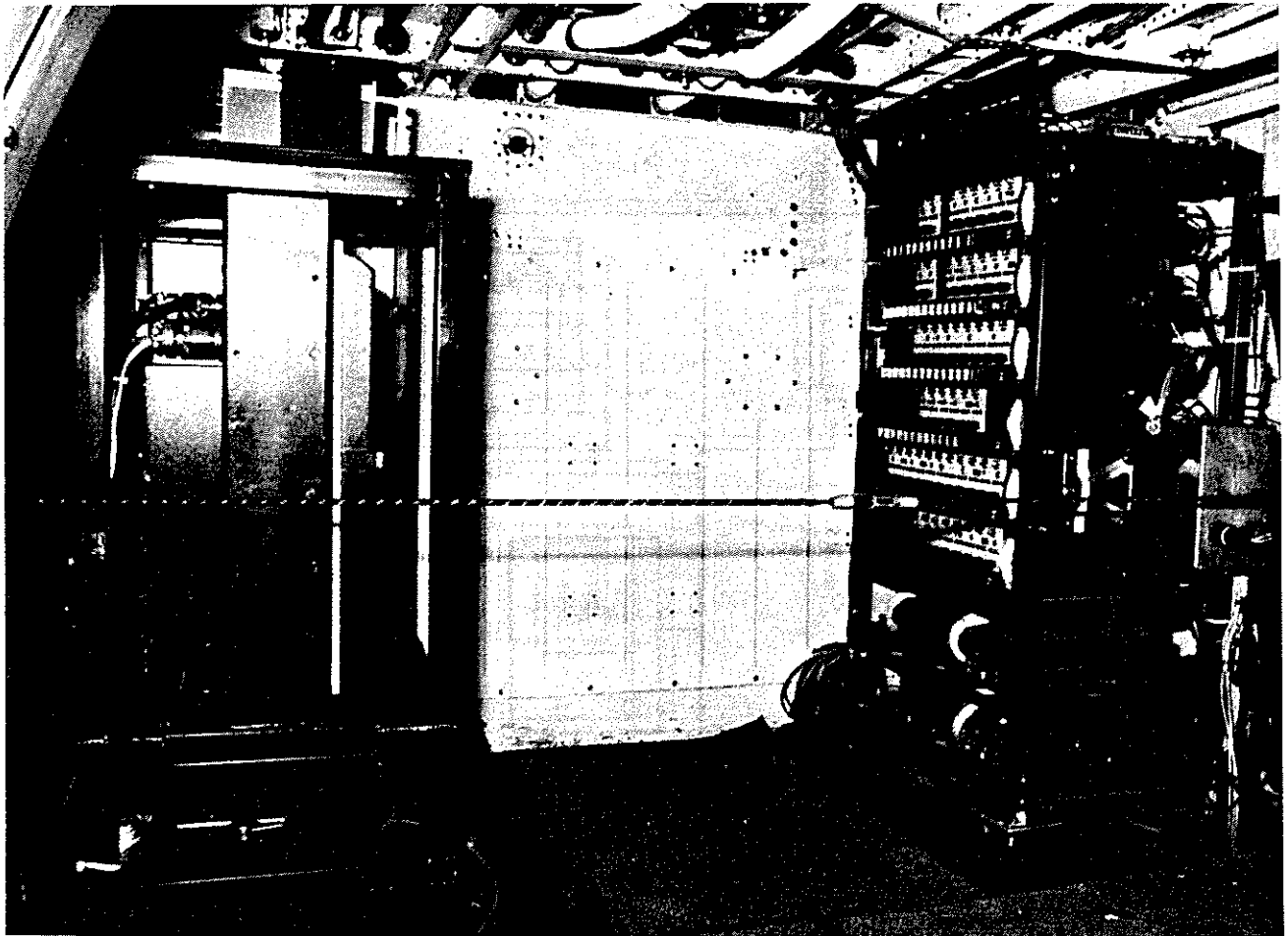


Figure 8 : AIRBORNE TEST UNIT

3.2 – Ground equipment

Telemetry unit

Fig. 10 describes this equipment. The operator has a VHF link to the helicopter being tested. His basic equipment consists of two scopes which receive and display the parameters being monitored and their limitations. (Although not shown here, he also receives the complete P.C.M. message, so he has a direct reading of flying control positions, speed, altitude, etc. . .).

The computing facilities here are merely analog analyzers which can give spectra of the signals received. Actually, because of the very short response time available to the operator, he mainly uses the scopes.

The photographs 11 and 12 show this room with its scopes, receiver and magnetic recorder.

Processing and analysis

During the test flight, but mainly after it, the data recorded on the on-board tape is analyzed by computer. Fig. 13 summarizes the various functions provided by a MITRA 125.

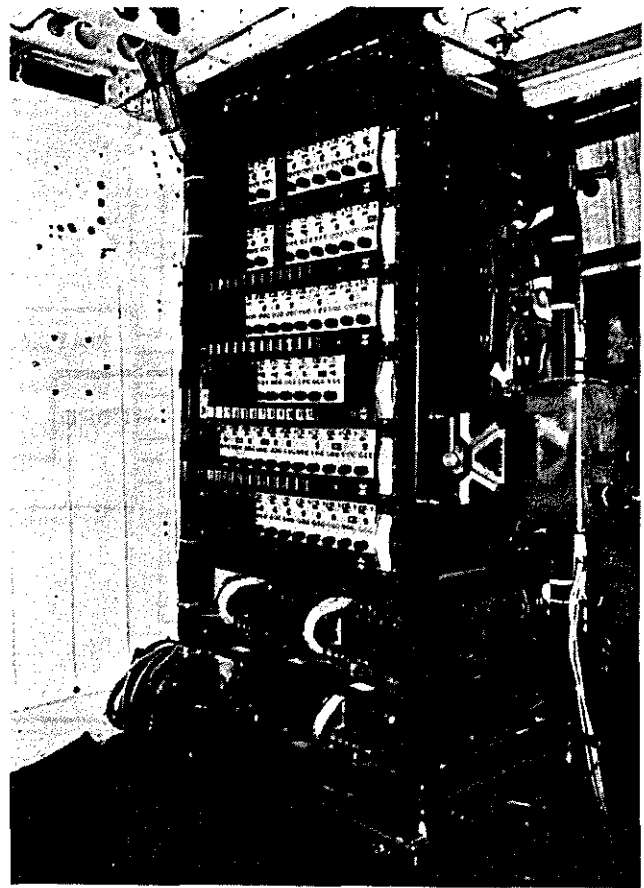


Figure 9 : AIRBORNE STRAIN GAUGE AMPLIFIERS

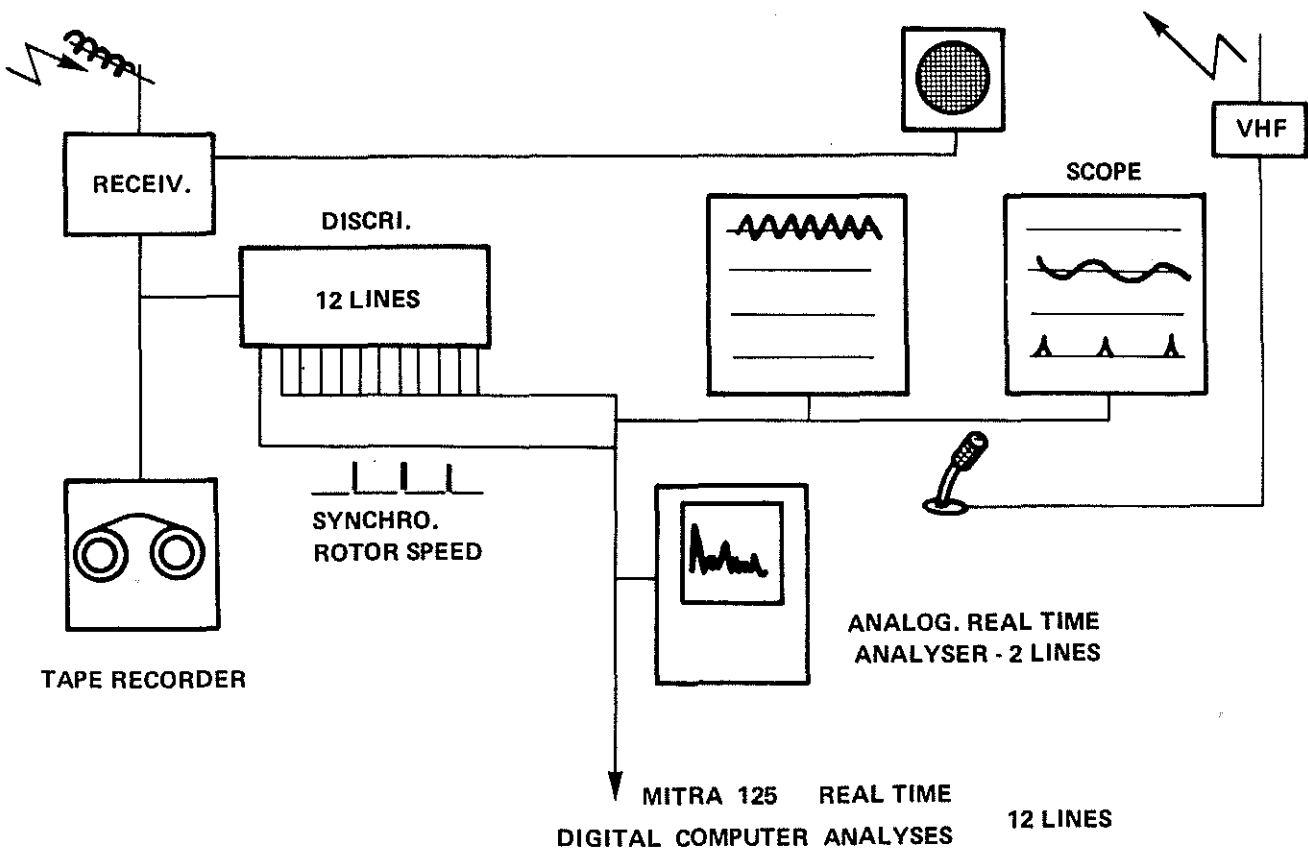


Figure 10 : BLOCK DIAGRAM OF GROUND TELEMETRICS EQUIPMENT

The data consists of the 12 tracks of a multiplex unit (which are processed in turn) and of a set of cards for calibration, two main stress levels or any other data required, such as the coded times of the sequences to be processed.

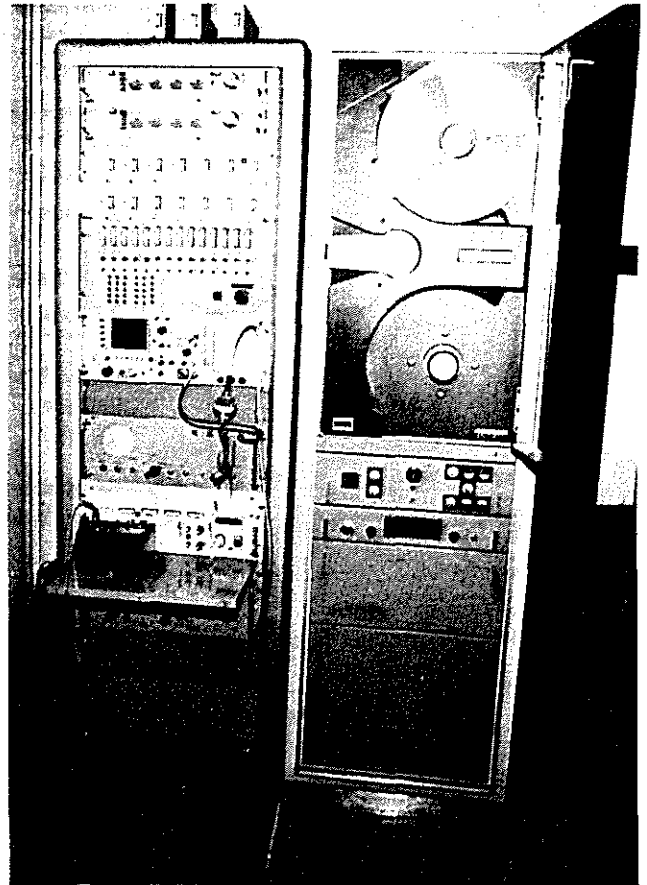
The memory contains three main programmes. The first two perform harmonic and spectral analyses and the third computes fatigue damage of the main components during typical flights. This data is used subsequently by the Engineering Dept. to calculate service life limits.

Of the possible outputs, magnetic tape is used mainly for storing the results of the 3 programmes, for subsequent statistic analysis.

The analysis outputs are either print-outs, plotter outputs or a hard copy "Tektronix" screen display.

Photographs 14, 15 and 16 give an impression of the data processing machine room (there are in fact two MITRA computers) with the peripherals.

One tends wherever possible to avoid digitized print-outs, which are tedious to process, and to obtain computed plots.



Figures 11 : TAPE READING UNIT

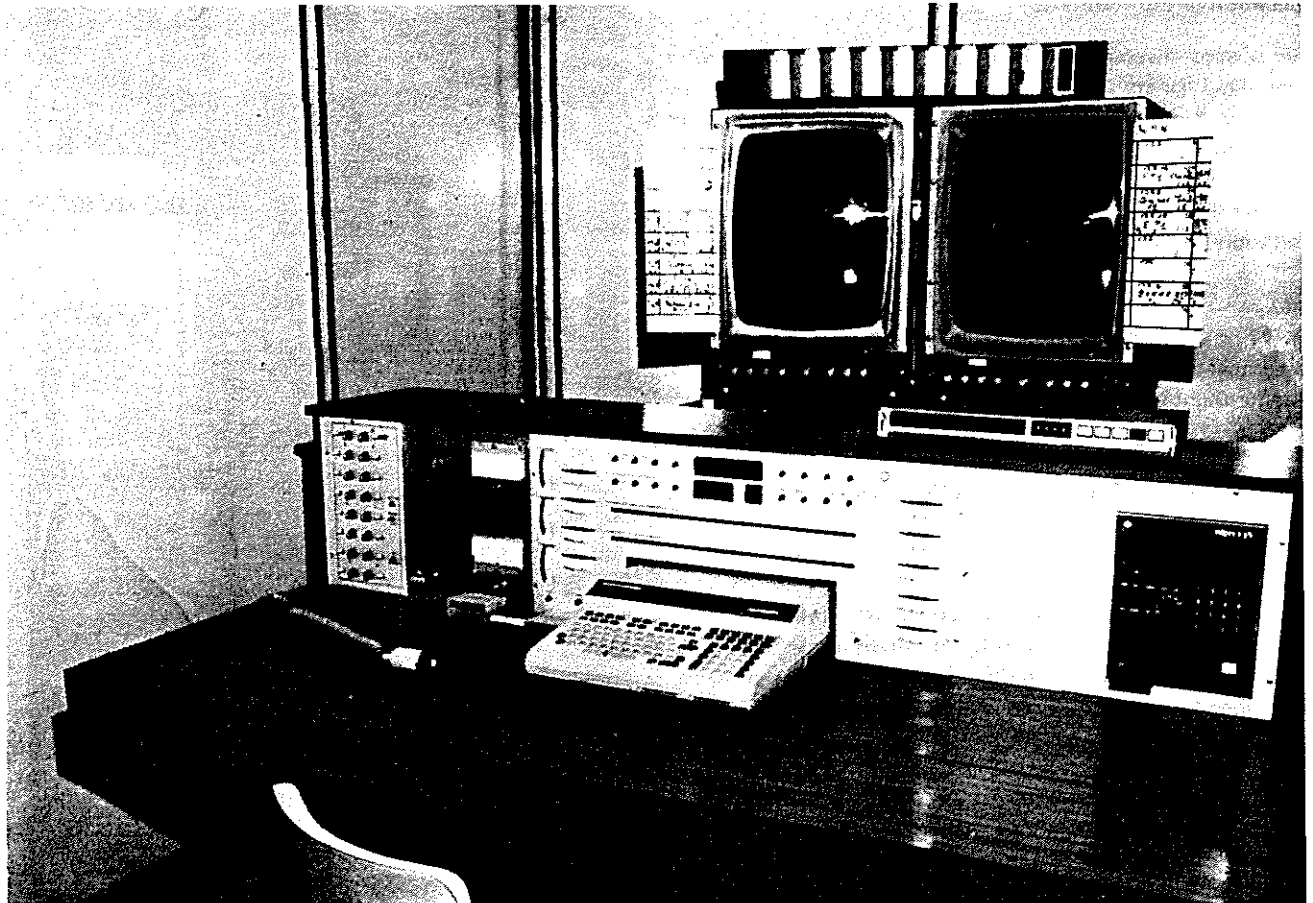


Figure 12 . TELEMETRIC DISPLAY UNIT (12 CHANNELS)

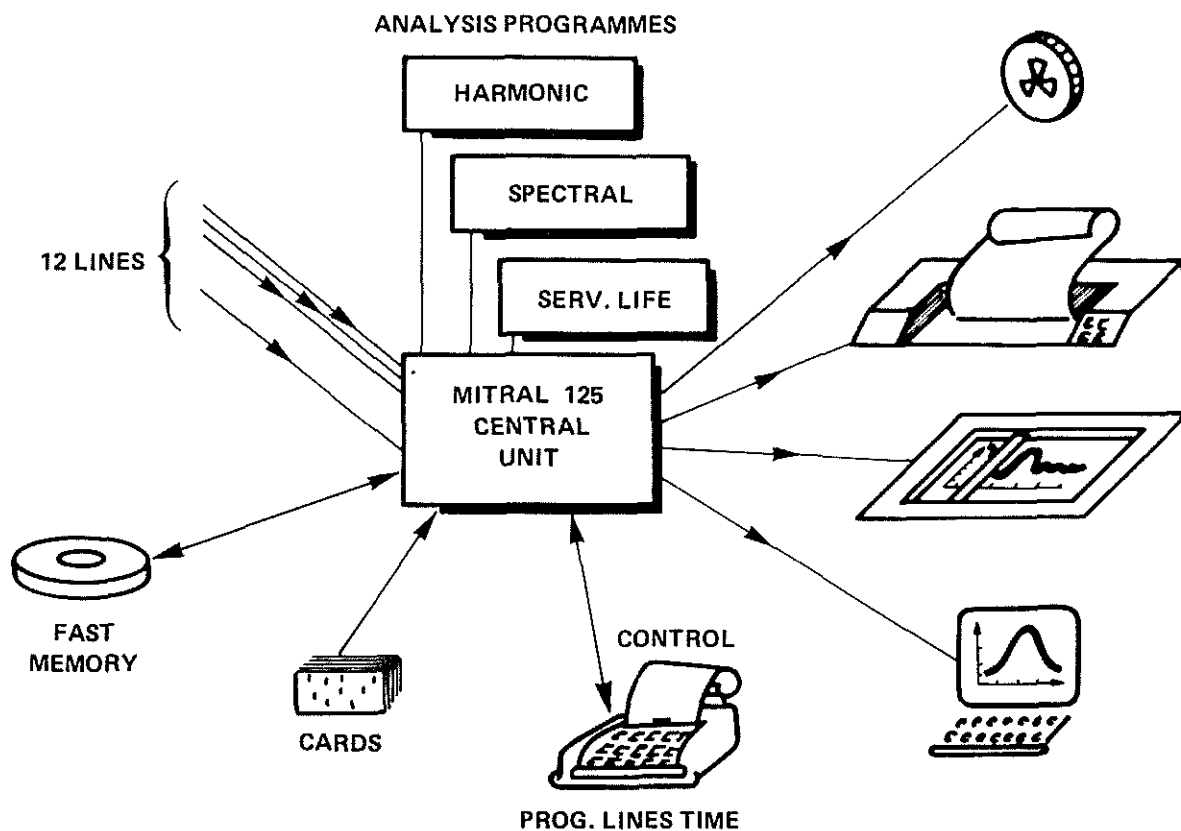


Figure 13 : BLOCK DIAGRAM OF GROUND COMPUTATION

Evaluation of test results

This always involves checking, first, the stress levels to ensure the safety of future flights, and secondly, the causes of high responses, that is, finding the spectrum areas containing the most energy. From then on, the aim is to move the blade's natural modes so as to reduce their response by setting them farther from the fundamental excitation frequencies.

Fig. 17 is a copy of a "Tektronix" screen hard copy providing the spectral analysis of a pitch control rod signal during a flight at different increasing speeds at 13 000 feet.

The analysis of such signals, both flapping and lagging, is used to establish the blade modes.

Fig. 18 shows a sample result of test stand vibration of a rotor, via the flying controls, at different rotor speeds. The advantage of this method is that, on the test stand, the phase and amplitude of the excitation are known.

Similar results are beginning to be obtained in flight by using more complex methods ; they are based on cross correlations between two parameters, which basically amounts to assuming that one is the source excitation and the other the response.

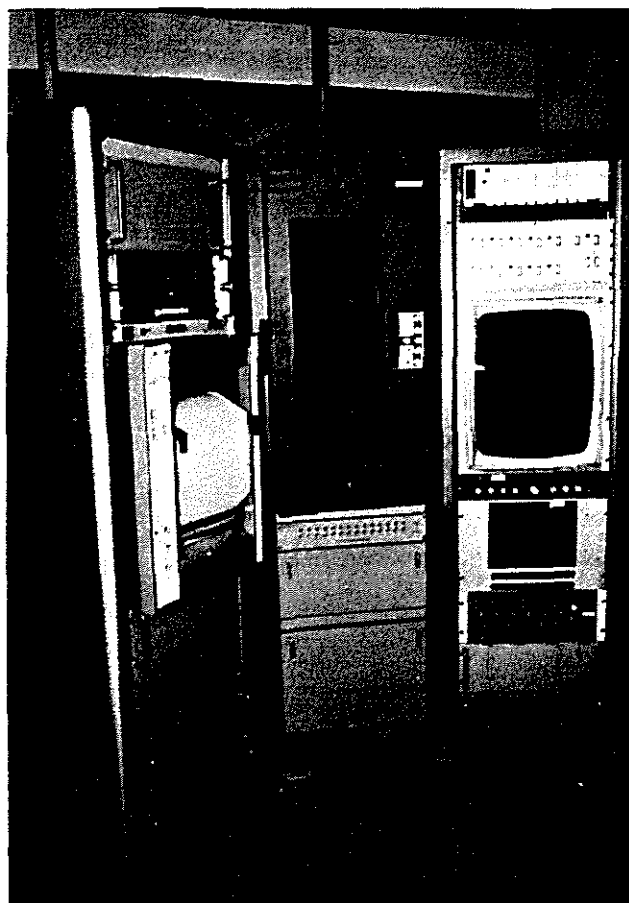


Figure 14 : TAPE CONTROLLER

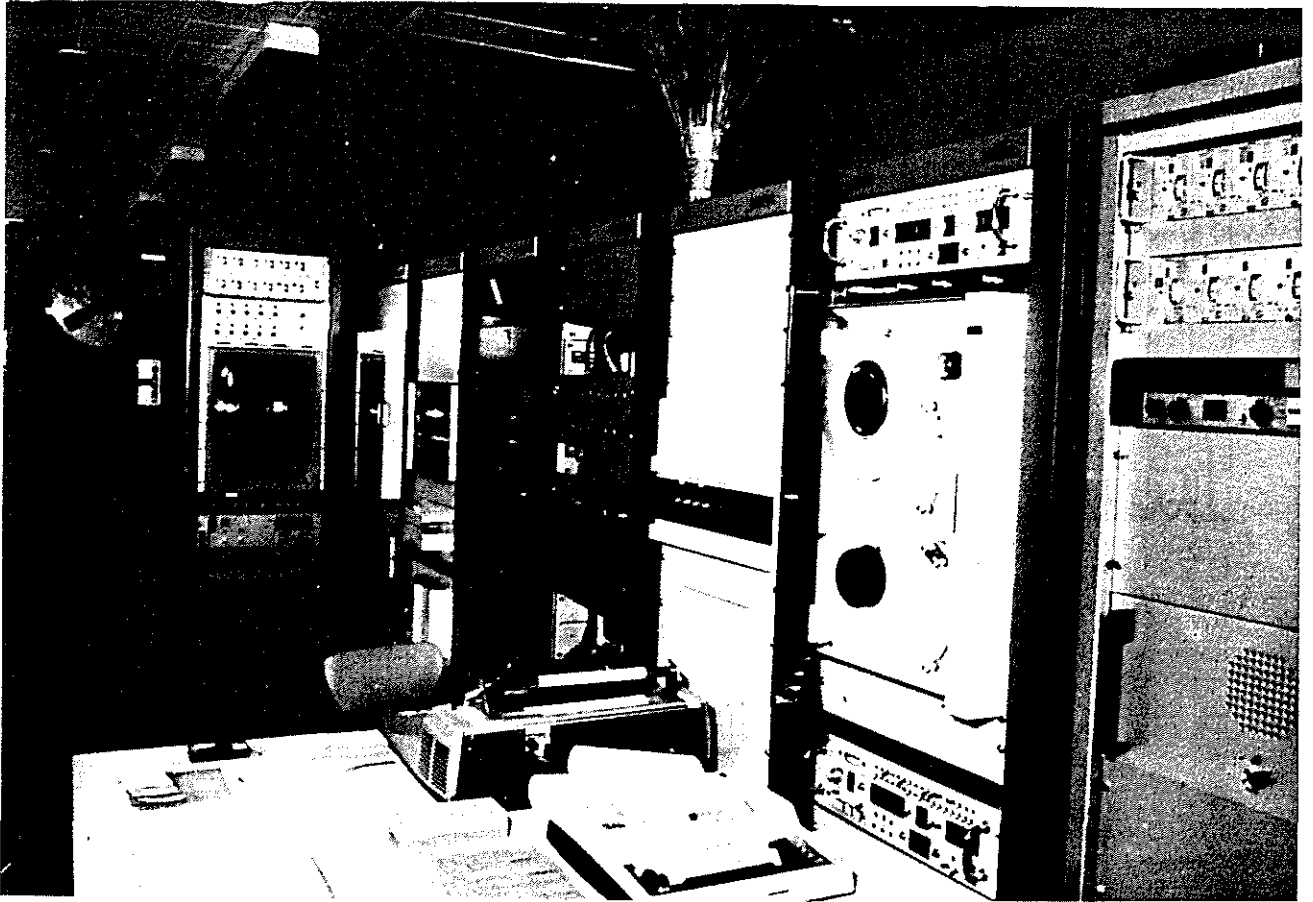


Figure 15 : DATA PROCESSING ROOM - GENERAL VIEW

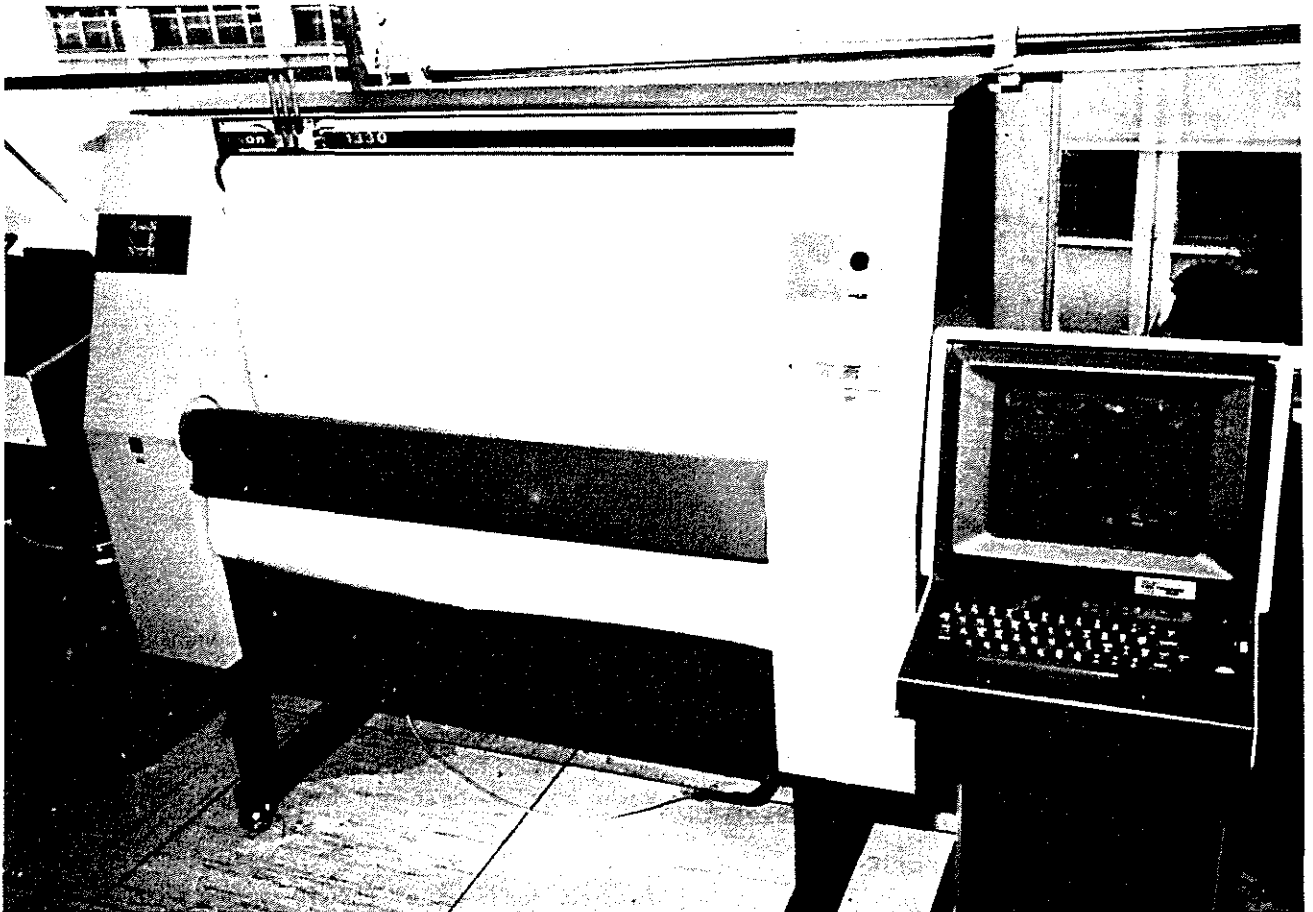


Figure 16 : DATA PRINTING UNIT

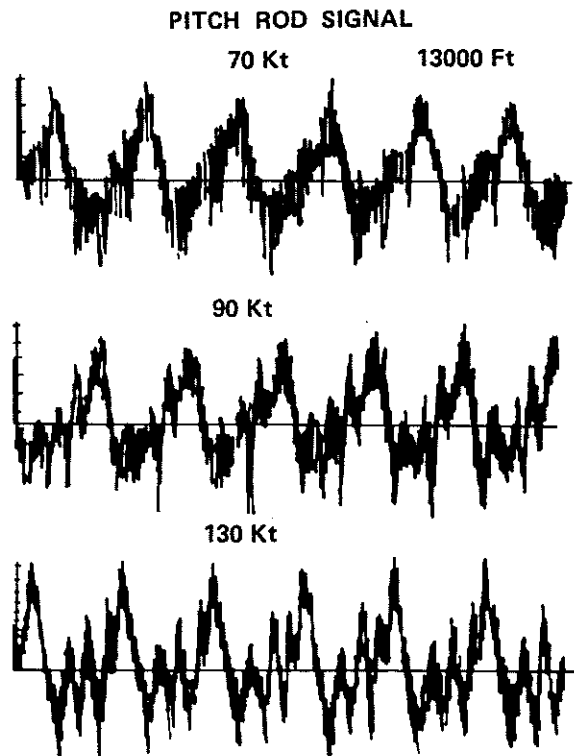


Figure 17 : SPECTRAL ANALYSIS OF PITCH CHANGE ROD SIGNAL

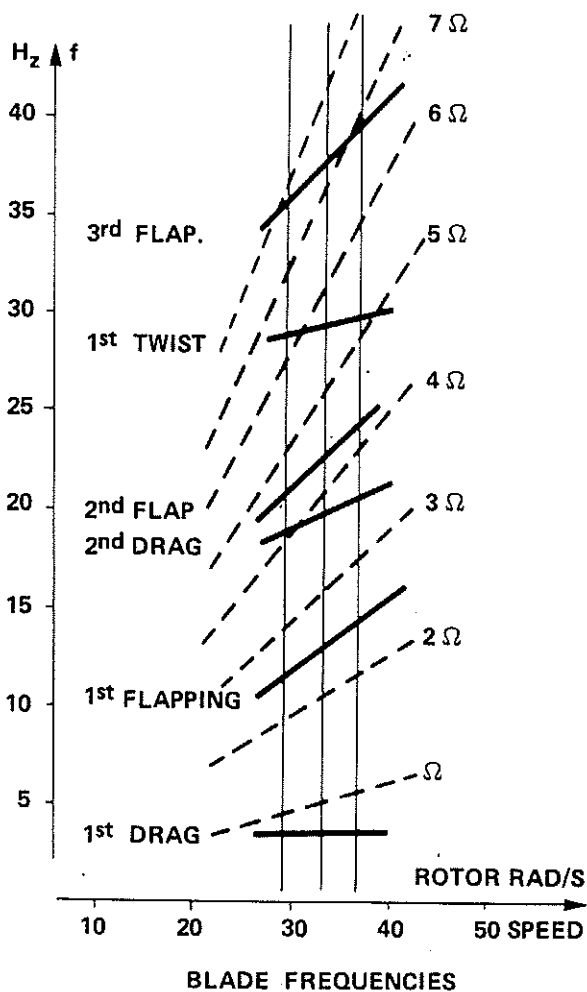


Figure 18 : CHART SHOWING NATURAL FREQUENCIES OF BLADES

When the cause, or presumed cause, of a problem has been identified, we still have to be able to effect appreciable modifications to the blades. Plastic blade technology is of great assistance here, because it is possible to achieve non-constant linear weight distributions by the addition of denser materials. Also, torsional rigidity can be adjusted by changing the laying angle of the skin layers of fibre cloth.

4 – TESTING METHODOLOGY

The flight envelope is extended progressively by dives at constant pitch, increasingly high speeds, low altitude and average weight levels. The weight is then increased up to the desired maximum. After that come the high altitude flights.

The process is the same for load factors ; testing is done at constant pitch and constant speed.

The difficulty of these tests lies in the complexity of their implementation (large number of parameters, fragility of gauges, variable calibration, interference. . .) and in the accurate performance of the test points, especially with respect to load factors, for which the speed of entering or leaving a turn can be an important parameter.

Accurate follow-up of aircraft configurations (weight, centre of gravity location) and of all modifications is essential, since their importance is not evident at first.

The Aerospatiale test teams are experienced in this type of testing, which requires unlimited confidence in the ground monitoring unit, which in fact has never yet let them down throughout the test flights for development and certification of a respectable number of helicopters over the last 20 years.

The fruits of this unceasing labour, to which all have contributed, can best be seen in the following figures for the 365N flight envelope as it stood in the early summer of 1980.

— Maximum weight : 3 850 kg.

At max. weight :

VD at low altitude : 183 kt

VD at 13,000 ft : 140 kt

Max. load factor at 140 kt, low altitude and max. continuous power : 1.8 g

Max. load factor at 100 kt, 13,000 ft and max. continuous power : 1.6 g.